

A SINGLE LAYER BIOFUEL CELL AS POTENTIAL COATING FOR IMPLANTABLE LOW POWER DEVICES

A. Kloke¹, B. Biller¹, S. Kerzenmacher^{1,*}, U. Kräling¹, R. Zengerle¹, and F. von Stetten¹

¹Laboratory for MEMS Application, Department of Microsystems Engineering - IMTEK, University of Freiburg, Georges-Koehler-Allee 106, 79110 Freiburg, Germany

*Corresponding author: Sven Kerzenmacher, +49-761-203-7328, FAX +49-761-203-7322, kerzenma@imtek.de

Abstract: Abiotically catalyzed glucose fuel cells were considered to only work with specific assemblies for electrode reaction separation. Using a highly porous oxygen tolerant catalyst for glucose oxidation we were able to realize a fuel cell with anode and cathode placed side by side. These results open the opportunity of having a sustainable power source implemented as single layer coating of medical implants. Further potential for power enhancement and cost reduction is identified within the variation of anode to cathode proportions.

Keywords: Biofuel Cell, Medical Implant, Implantable Power Source

INTRODUCTION

Abiotically catalyzed glucose fuel cells represent a fully self-sufficient approach to supply low power medical implants within the human body [1]. These fuel cells gain electrical energy by the separated electrochemical conversion of dissolved oxygen and glucose from body fluids (see Fig. 1).

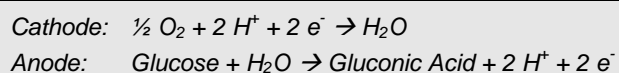


Figure 1: Predominant electrode reactions in an abiotically catalyzed glucose fuel cell

As a future replacement of batteries in implanted medical microdevices glucose fuel cells are favorable to mechanical energy harvesting systems because of their continuous and thus more reliable power generation. Compared to biocatalysts such as enzymes or microorganisms, abiotic catalysts promise long-term stability, simple sterilization procedure and thus biocompatibility, but are less specific toward the conversion of glucose.

Such a fuel cell can be applied as exterior coating of implant capsules. Early works already demonstrated the tissue implantability of such a fuel cell device under in-vivo conditions in a dog [2]. In-vitro, power densities of about $3.3 \mu W cm^{-2}$ are reported for initial operation, and $1 \mu W cm^{-2}$ for long-term performance [3]. Considering that nowadays a cardiac pacemaker demands about $8 \mu W$ [4], a fuel cell of $4 cm^2$ coated to each side of a pacemaker capsule would thus already be sufficient for operation.

Most noble metal catalyst used for glucose oxidation are also catalytically active towards oxygen reduction. Consequently, the simultaneous presence of glucose and oxygen in body fluids demands for a separation of reactants, to avoid oxygen interference at the anode. This would lead to a more positive anode potential and thus lower the overall cell voltage.

In literature, several stacked fuel cell designs are suggested to overcome this problem [2, 5]. For

instance Rao et al. suggest mounting an oxygen consuming cathode in front of the anode [5] (Fig. 2A). This is to establish nearly anoxic conditions at the anode for electrochemical oxidation of glucose.

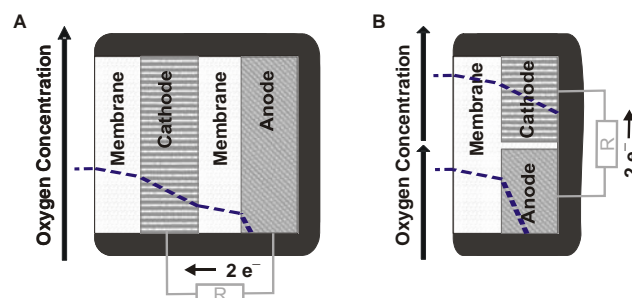


Figure 2: Glucose Fuel Cell Designs: (A) Stacked assembly suggested by Rao et al. [5]; (B) Single layer layout with anode and cathode placed side by side. The dashed line qualitatively indicates the progression of the oxygen concentration inside the fuel cell.

In this work we report on the oxygen-tolerance of our recently presented Pt-Zn anodes [6], and present a corresponding single layer fuel cell with equally sized anode and cathode operated side by side (Fig. 2B). Based on the experimental results we propose the variation of anode to cathode proportion as opportunity for further power enhancement and cost reduction.

ELECTRODE FABRICATION

Both platinum based electrodes were fabricated using a thermal alloying process followed by chemical dissolution of the alloy partner for the creation of a highly rough platinum catalyst surface. Pt-Zn anodes were prepared from $50 \mu m$ thick platinum foils ($1.5 \times 1.5 cm^2$) and an electrodeposited $30 \mu m$ thick layer of zinc corresponding to the procedure described in [6]. After annealing (48 h, $200^\circ C$) the remaining zinc, which is not involved in alloy formation, is removed in $0.5 mol l^{-1} H_2SO_4$.

For Pt-Al cathodes 20nm of titanium and subsequently 500 nm of each platinum and aluminum are evaporated onto a silicon substrate (1.5 x 1.5 cm²). Aluminum as sacrificial alloy partner is removed after annealing (1h, 300°C) in 1 mol l⁻¹ NaOH, comparable to the procedure described in [7].

CHARACTERIZATION METHODS

In preliminary experiments it has been observed that oxygen concentration has a more distinct effect on the anode open circuit potential than on the polarization curve.

We therefore focused on the open circuit potential to investigate the oxygen sensitivity of the anode potential. Thereto equilibrium values for open circuit potentials (OCV, 0 μA cm⁻²) in phosphate buffered saline (PBS tabs pH = 7.4, Invitrogen GmbH, Karlsruhe, Germany) with different glucose and oxygen concentrations have been determined. Oxygen saturation was varied within the physiological range (up to 7 %). Glucose concentrations of 0.5 and 2.5 mmol l⁻¹ were chosen for this investigation. This is slightly lower than the 3 to 4 mmol l⁻¹ reported for interstitial fluid [8] to account for the diminished glucose availability expected from tissue encapsulation.

Each equilibrium value was calculated from four day potential monitoring of three to four electrodes. Between measurements at different oxygen concentrations the anodes were regenerated to exclude aging effects. This was done by cyclic voltammetry conducted under nitrogen atmosphere (10 cycles between -0.9 V and 1.4 V vs. SCE with a scan speed of 10 mV s⁻¹).

Fuel cell experiments were performed at 7% oxygen saturation which is the maximum oxygen concentration reported for tissue [9] and a glucose concentration of 3 mmol l⁻¹ in PBS. A Supor-450 membrane filter (0.45 μm pore size, Pall Life Sciences, USA) was mounted on top of the fuel cell to experimentally simulate tissue encapsulation. It exhibits a similar diffusion resistance for glucose as the tissue capsule forming around implanted devices [10]. Starting from OCV (0 μA cm⁻²), the galvanostatic load is stepwise increased to values of 4.43 μA cm⁻², 8.95 μA cm⁻², 13.45 μA cm⁻² and 17.97 μA cm⁻². For the construction of polarization curves the stable electrode potentials after 12 hours of operation at a given load were taken.

In all experiments, a stimulus generator (STG 2008, Multichannel Systems, Reutlingen, Germany) was used as galvanostat in combination with a data acquisition system (Keithley 2700, Keithley, Germering, Germany). Electrode potentials were recorded against a saturated calomel reference electrode (SCE; KE11, Sensortechnik Meinsberg GmbH, Ziegra-Knobelsdorf, Germany). Oxygen concentrations were set using a gas proportioner (ANALYT-MTC GmbH & Co KG, Müllheim, Germany) with air and nitrogen. All measurements were conducted at 37°C.

OXYGEN TOLERANCE OF Pt-Zn ELECTRODES

The influence of oxygen concentration on the electrode potential of Pt-Zn anodes at two different concentrations of glucose is shown in Fig. 3.

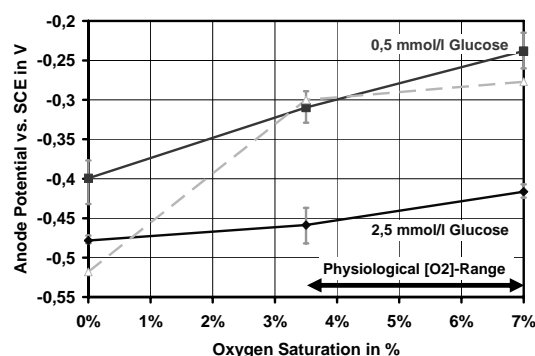


Figure 3: Equilibrium anode open circuit potentials are presented for Pt-Zn anode at different glucose and oxygen concentrations (solid lines). Comparable data for a state-of-the-art anode in a stacked fuel cell design (extracted from [3], 5 mmol l⁻¹ glucose) is plotted as dashed line.

For 2.5 mmol l⁻¹ glucose the anode potential at 7 % oxygen saturation increases by only 60 mV compared to anoxic conditions (0 % oxygen saturation). For 0.5 mmol l⁻¹ glucose concentration an increase of 160 mV is observed. For the state-of-the-art anode the potential strongly increases by 320 mV from 0 % to 3.5 % oxygen saturation, and by only 30 mV from 3.5 % to 7 %.

These observations clearly demonstrate for Pt-Zn anodes that the increase in anode potential with increasing oxygen concentration is reduced at higher glucose concentrations. Furthermore Pt-Zn anodes show an increased overall oxygen tolerance compared to state-of-the-art, even when operated at lower glucose concentrations.

To evaluate the magnitude of the here obtained differences in anode potential we calculated corresponding fuel cell voltages. A single layer biofuel cell cathode has an open circuit potential of 250 mV at 7 % oxygen saturation (see Fig. 5). When the anode is operated under anoxic conditions a cell voltage of 730 mV and 650 mV is obtained for glucose concentrations of 2.5 mmol l⁻¹ and 0.5 mmol l⁻¹, respectively. At 7% oxygen saturation at the anode the cell voltage is reduced by 8 % for 2.5 mmol l⁻¹ and 25 % for 0.5 mmol l⁻¹ glucose concentrations. For the shown state-of-the-art electrode (5 mmol l⁻¹ glucose) a significantly stronger reduction in cell voltage of 45 % is obtained.

Furthermore, even in the absence of oxygen a general dependence of the Pt-Zn anode's open circuit potential on glucose concentration is observable. At 2.5 mmol l⁻¹ glucose an about 80 mV more negative potential is obtained than at 0.5 mmol l⁻¹ glucose.

SINGLE LAYER BIOFUEL CELL: RESULTS

Utilizing the oxygen tolerance of the Pt-Zn anodes, a fuel cell without stacking is assembled by placing anode and cathode side by side. The polarization curve of this single layer biofuel cell is presented in Fig. 4. The open circuit potential amounts to 630 mV. At current densities above $9 \mu\text{A cm}^{-2}$ an accelerated decrease in cell voltage is observed, and at about $17 \mu\text{A cm}^{-2}$ the cell voltage finally drops to zero.

The resulting power output, normalized to the total fuel cell area, is also shown in Fig. 4. A maximum power density of $2.0 \mu\text{W cm}^{-2}$ is achieved at a current density of $8.95 \mu\text{A cm}^{-2}$.

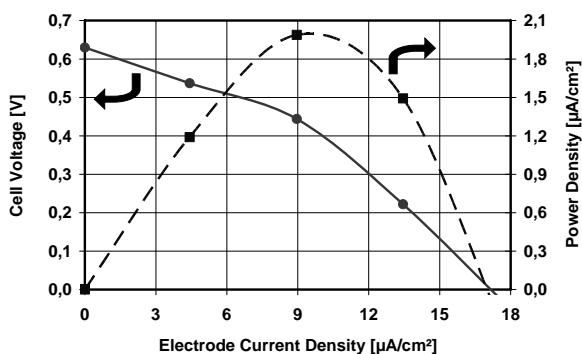


Figure 4: Cell voltage and power density of a single layer fuel cell operated at 37°C in PBS with 3 mmol l^{-1} glucose and 7 % oxygen saturation. Current density is normalized to the area of the individual electrodes whereas power density is referred to the total fuel cell area.

In Fig. 5 individual load curves for anode and cathode of the presented single layer biofuel cell are shown, recorded against an SCE reference electrode. The anode's OCV is slightly more positive than what is expected from Fig. 3. This is because within this investigation unlike as in Fig. 3 potential values were taken after a stabilization time of only 12 hours.

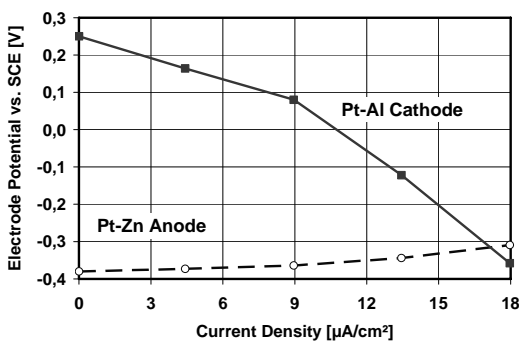


Figure 5: Load curves for anode (dashed line) and cathode (solid line) of a single layer fuel cell in PBS with 3 mmol l^{-1} glucose and 7 % of oxygen saturation

For currents densities above $9 \mu\text{A cm}^{-2}$ cathode potential does not follow the linear (ohmic) behavior of the lower current density regime anymore. Here the cathode reaction becomes subject to mass transport limitations due to the low concentration of dissolved oxygen.

In general, the cathode shows a much stronger polarization than the anode. From the slope of the electrode polarization curves between $4.43 \mu\text{A cm}^{-2}$ and $8.95 \mu\text{A cm}^{-2}$ (ohmic region) an average ohmic polarization (area specific resistance) of $-18.6 \text{ k}\Omega \text{ cm}^2$ and $2.0 \text{ k}\Omega \text{ cm}^2$ can be extracted for cathode and anode, respectively. This means that cathode polarization is 9.3 times larger than that of the anode. Thus the overall cell voltage decay is primarily due to cathode polarization.

SINGLE LAYER BIOFUEL CELL: DISCUSSION

For the single layer fuel cell we found a power density of $2.0 \mu\text{W cm}^{-2}$. This is only about 40 % less than the $3.3 \mu\text{W cm}^{-2}$ reported for a stacked activated carbon based biofuel cell [3]. Furthermore the fuel cell cited here was tested under conditions (21% oxygen saturation, 5 mmol l^{-1} glucose) at which even higher power densities can be expected.

In stacked fuel cells equally sized electrodes are placed onto each other, resulting in a total fuel cell area reduced by the factor of 2. To compare the electrode performance we therefore need to double the power density achieved for the single layer fuel cell. This way, a power output per electrode area of $4.0 \mu\text{W cm}^{-2}$ is calculated for the single-layer fuel cell. This is a $0.7 \mu\text{W cm}^{-2}$ higher power density compared to the cited state-of-the-art fuel cell. However, this improvement is mainly due to the different electrode materials, and cannot be ascribed to the changed fuel cell design.

Hence, the shown fuel cell results clearly demonstrate that an oxygen consuming layer in front of the anode is not essential to operate a biofuel cell.

ELECTRODE PROPORTION VARIATION

As shown in Fig. 5, the strong decrease in cathode potential was identified as main reason for the fast overall decay of cell voltage (see Fig. 5). To balance this one can take advantage of an opportunity not applicable for stacked assemblies: variation of cathode to anode area proportions. We therefore utilized the above derived average ohmic polarizations (given per electrode area) to calculate cell voltages and thus power densities for fuel cells having the same total area, but different electrode proportions.

Fig. 6 displays the maximum power densities achievable for different ratios of cathode to anode area from 0.1 to 15. Considering the calculated value for ratio 1 a value of $2.4 \mu\text{W}$ is found, which is about 20% higher than the experimentally determined value (see Fig. 4). The calculated maximum power density in this case cannot be reached because at the required current density of

16.0 $\mu\text{A cm}^{-2}$ the cathode potential will already be superimposed by mass transport limitations. An overall maximum is found for a cathode to anode ratio of about 3. For this combination a power density of 3.0 $\mu\text{W cm}^{-2}$ is predicted. This implies a possible power density enhancement by 50 % compared to the experimentally determined maximum power density for ratio 1. The predicted maximum power density requires a cathode current density of 12.0 $\mu\text{A cm}^{-2}$. Unfortunately, this is already in the current density regime in which the cathode becomes subject to mass transport limitations. Accordingly, one would probably find a slightly lowered power density if doing the corresponding experiment.

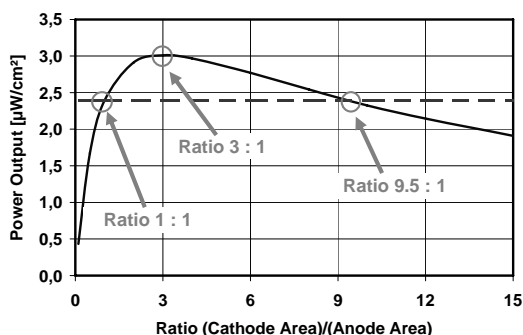


Figure 6: Calculated maximum power densities with varying ratios of cathode to anode areas. The dashed line indicates maximum power densities predicted for equally sized anode and cathode.

Another interesting ratio is 9.5. Here the same power output is achieved compared to ratio 1, but with about only 10 % of anode proportion within the fuel cell. This power output is achieved at a cathode current density of 7.7 $\mu\text{A cm}^{-2}$ and thus won't be limited by diffusive limitations. Due to the 50 μm thick platinum foil required for its fabrication, the anode is significantly more expensive than the cathode fabricated from evaporated metal layers. Consequently, changing the anode to cathode proportions from 1 to 9.5 allows for a cost reduction up to a factor of 5.

To understand the appearance of the points marked in Fig.6 one needs to calculate the electrode polarization slopes for corresponding area proportions. For ratio 9.5 one obtains a cathode to anode polarization ratio of 1/9.5 what is the inverse of the experimentally found ratio for equally sized electrodes. Therefore the same power density is achieved as with ratio 1. In case of the overall maximum at ratio 3 anode and cathode have equal polarization slopes, leading to the overall maximum power density.

CONCLUSIONS

An improved oxygen-tolerance is found for Pt-Zn anodes as compared to state-of-the-art. The open circuit cell voltages become thus reduced by only 8-25 % for Pt-Zn anodes instead of 45 % for state-of-the-art anodes, if oxygen saturation is increased

from 0 % to 7 %. Accordingly we can qualify Pt-Zn anodes to be tolerant, but not insensitive towards oxygen.

We obtained a fairly high maximum power density of 2.0 $\mu\text{W cm}^{-2}$ for the presented single layer biofuel cell. Consequently the experiments demonstrate that layer stacking and the hereby created oxygen depletion at the anode is not essential for the operation of a glucose fuel cell. Hence, placing electrodes side by side is a way to circumvent stacking and thus facilitate fuel cell integration on implant capsules.

Furthermore we introduced variation of electrode area proportions of cathode and anode as a means to further enhance power density of single layer fuel cells by up to 50 %, or to strongly reduce their costs. For a cathode to anode area ratio of 3 a power density of 3.0 $\mu\text{W cm}^{-2}$ is predicted, only 10 % lower than reported for stacked fuel cells.

In our current work we assemble single layer biofuel cells with varied cathode to anode ratios to experimentally proof our predictions.

ACKNOWLEDGEMENT

We gratefully acknowledge financial support from the German Research Association DFG (GR1322) and the EU (contract No. 001837 Healthy Aims).

REFERENCES

1. F. Von Stetten, S. Kerzenmacher, R. Sumbharaju, R. Zengerle, J. Ducreé; Proceedings of the, EUROSENSORS XX Conference 2006, p. M2C-KN
2. R.F. Drake, B.K. Kusserow, S. Messinger, S. Matsuda, Trans. Amer. Soc. Artif. Organs 16 (1970) p. 199-205
3. S. Kerzenmacher, J. Ducreé, R. Zengerle, F. von Stetten; Journal of Power Sources 182 (2008), p. 66-75
4. L.S.Y. Wong, S. Hossain, A. Ta, J. Edvinsson, D.H. Rivas, H. Naas, IEEE J. Solid-State Circuits 39 (2004), p 1079-1083
5. J.R. Rao, G. Richter, F. von Sturm, E. Weidlich; Berichte der Bunsen-Gesellschaft – Phys.1 Chem. Chem. Phys., 77 (1973), p 787-790.
6. S. Kerzenmacher, J. Ducreé, R. Zengerle, F. Von Stetten; Proceedings of 7th Power MEMS 2007, p. 31-34
7. P.D. van der Wal, M. Dadrás, M. Koudelka-Hep, N.F. de Rooij; Abstract of the 206th Meeting of the ECS, p. 495
8. D.G. Maggs, R. Jacob, F.Rife, R. Lange, P. Leone, M.J.During, W.V. Tamborlane, R.S. Sherwin; J. Clin. Invest. 96 (1995), p. 370-377
9. D.A. Gough, F.L. Anderson, J.Giner, C.K. Colton, J.S. Soeldner; Anal. Chem. 50(1978), p. 941-944
10. A.A. Sharkawy, B. Klitzman, G.A. Truskey, W.M. Reichert, Journal of Biomedical Materials Research 37 (1997), p. 401-412